Universal Low-Frequency Vibrational Modes in Silica Glasses

Silvia Bonfanti,[1] Roberto Guerra ©,[1] Chandana Mondal,[2] Itamar Procaccia,[2,3] and Stefano Zapperi[1,4]

[1]*Center for Complexity and Biosystems, Department of Physics, University of Milan, via Celoria 16, 20133 Milano, Italy*
[2]*Department of Chemical Physics, The Weizmann Institute of Science, Rehovot 76100, Israel*
[3]*Center for OPTical IMagery Analysis and Learning, Northwestern Polytechnical University, Xi'an, 710072 China*
[4]*CNR—Consiglio Nazionale delle Ricerche, Istituto di Chimica della Materia Condensata e di Tecnologie per l'Energia,*
Via R. Cozzi 53, 20125 Milano, Italy

It was recently shown that different simple models of glass formers with binary interactions define a universality class in terms of the density of states of their quasilocalized low-frequency modes. Explicitly, once the hybridization with standard Debye (extended) modes is avoided, a number of such models exhibit a universal density of states, depending on the mode frequencies as $D(\omega) \sim \omega^4$. It is unknown, however, how wide this universality class is, and whether it also pertains to more realistic models of glass formers. To address this issue we present analysis of the quasilocalized modes in silica, a network glass that has both binary and ternary interactions. We conclude that in three dimensions silica exhibits the very same frequency dependence at low frequencies, suggesting that this universal form is a generic consequence of amorphous glassiness.

Introduction.—Theoretical considerations pointed out for quite some time [1–4] that low-frequency vibrational modes in amorphous glassy systems are expected to present a density of states $D(\omega)$ with a universal dependence on the frequency ω, i.e.,

$$D(\omega) \sim \omega^4. \tag{1}$$

In spite of the fact that numerical simulations of a variety of model glass formers proliferated in recent years, the direct verification of this prediction was late in coming. The reason for this is that the modes which are expected to exhibit this universal scaling are quasilocalized modes that in large systems hybridize strongly with low frequency delocalized elastic (Debye) extended modes, whose density of states is expected to depend on frequency like ω^{d-1} where d is the spatial dimension. To observe the universal scaling Eq. (1) one needs to disentangle these types of modes. A simple and successful idea was presented in Ref. [5], using the fact that low frequency Debye modes have a lower cutoff that is determined by the system size. By analyzing small enough systems one could isolate the relevant quasilocalized modes and their density of states, keeping the lowest available Debye mode cleanly above the observed frequency range.

Other methods and models were introduced to examine the density of states of the glassy modes. For example, Baity-Jesi *et al.* computed the inherent structures in a Heisenberg spin glass in a random field by diagonalizing the Hessian matrix [6] while a similar method was employed by Shimada *et al.* for a three-dimensional packing of particles interacting via short-ranged harmonic interactions [7]. Moriel *et al.* studied the attenuation of long-wavelength phonons by glassy disorder using theory and simulations of a set of bidisperse particles with repulsive interactions [8] and a similar model was analyzed in Ref. [9].

Invariably, the demonstration of the universal frequency dependence Eq. (1) was limited so far to models with binary interaction only [10,11]. The theoretical analysis of Refs. [1–4] is, however, much more general, describing low frequency glassy modes as resulting from soft oscillators in the neighborhood of stiffer ones, and with long-range interactions between the soft oscillators. It is therefore timely and relevant to examine whether the universality class extends to glass formers of more realistic interactions [12]. Here we present results for silica glass which has both binary and ternary interactions. We need to find below how to avoid the influence of low lying Debye modes, and discuss how to choose the system size to explore the density of quasilocalized modes.

System and protocols.—Our model of silica glass is simulated in three-dimensional cubic boxes for three different system sizes: (i) $N = 222$ atoms composed by $N_{Si} = 74$ silicon atoms and $N_O = 148$ oxygen atoms. Box length $L = 15$ Å, 1000 configurations. (ii) $N = 1032$ atoms composed by $N_{Si} = 344$ silicon atoms and $N_O = 688$ oxygen atoms. Box length $L = 25$ Å, 1000 configurations. (iii) $N = 4008$ atoms composed by $N_{Si} = 1336$ silicon atoms and $N_O = 2672$ oxygen atoms. Box length $L = 39.3$ Å, 250 configurations.

The interaction between atoms is given by the Watanabe's potential [13] following Refs. [14,15].

Details on the potential and parameters used are reported for completeness in the Supplemental Material [16]. Units in the following are defined on the basis of energy, length, and time, being eV, Å, and ps, respectively. The preparation protocol starts with randomly positioned Si,O atoms, with density $\rho_{in} = 2.196$ g/cm^3, followed by an annealing procedure: (1) After an initial 2 ps of Newtonian dynamics with Lennard-Jones interatomic interactions, viscously damped with a rate of 1/ps and atomic velocities limited to 1 Å/ps, we switch to our reference Watanabe's potential for silica [13]. (2) We perform subsequent 8 ps of damped Newtonian dynamics. (3) We then heat up the system up to 4000 K and then quench to 0 K in 100 ps, corresponding to a cooling rate of 40 K/ps. (4) The so-produced configurations are then minimized through the fast inertial relaxation engine (FIRE) [17] until the total force on every atom satisfies $|\mathbf{F}_i| \leq 10^{-10}$ eV/Å.

Notice that we use rather fast cooling rates. Slower cooling rates are typically used in experiments but difficult to achieve numerically. Previous simulations in a simpler glass model show that the universal features of the vibrational spectrum do not depend on the cooling rate [5]. Furthermore, by construction, the density of our samples compares well with experimentally observed values [18] and with previous calculations of atomic coordination [19].

The low frequency vibrational modes.—Denote as $U(\mathbf{r}_1, \mathbf{r}_2, \cdots \mathbf{r}_N)$ the total potential energy of the system with $\{\mathbf{r}_i\}_{i=1}^N$ being the coordinates of the particles. As usual [20–22], the modes of the system in athermal conditions $(T = 0)$ are obtained by diagonalizing the Hessian matrix [23]:

$$H_{ij}^{\alpha\beta} \equiv \frac{\partial^2 U(\mathbf{r}_1, \mathbf{r}_2, \cdots \mathbf{r}_N)}{\partial r_i^\alpha \partial r_j^\beta} = -\frac{\partial F_i^\alpha}{\partial r_i^\beta}. \qquad (2)$$

The mode frequencies ω are obtained by the square root of the Hessian eigenvalues, and we define ω_{min} as the lowest frequency after removing the three translational zero modes. The eigenvectors provide information on which modes are localized and which are not, as seen below. In our simulations, the Hessian matrix is computed numerically from the first-order derivatives of inter-particle forces, cf. Eq. (2). Each element $H_{ij}^{\alpha\beta}$ is obtained by calculating the force F_i^α on particle i resulting from a displacement of particle j by a small amount, $\Delta(r_j^\beta) = 10^{-7}$ Å along positive and negative β direction, and by applying the difference quotient. All the simulations have been performed using the LAMMPS simulator package [24], and visualized with the OVITO package [25].

Results.—In Fig. 1 we report the density of states for the lowest frequencies in each of the three simulated system sizes. In general we see that the predicted power law ω^4 fits very well the low frequencies tail. Interestingly, for the smallest system with $N = 222$ the power law extends
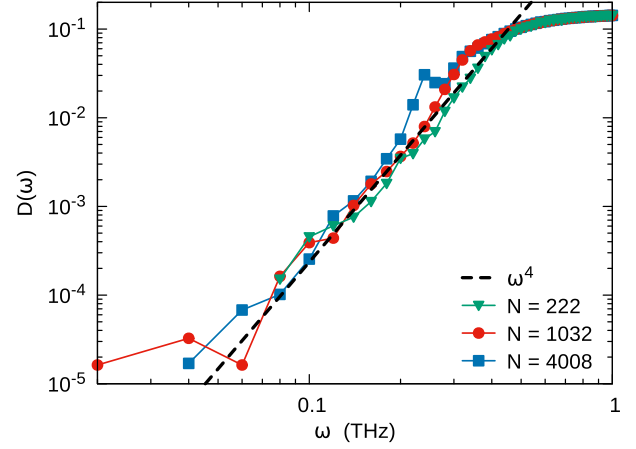

FIG. 1. Density of vibrational modes $D(\omega)$ (circles) for three different system sizes. The dashed line represents the scaling law $D(\omega) \propto \omega^4$. One learns that the scaling law is obeyed with a diminishing range when the system size increases. It is shown below that this is due to invasion of the low frequency range by extended phonon modes that can hybridize with the quasilocalized modes.

throughout, whereas for the larger two systems we see the peak belonging to elastic modes sneaking in from above, invading lower frequencies for the largest system with $N = 4008$. To substantiate this, we computed the participation ratio associated with the modes in the pure power law regime and with modes whose frequency is larger than 0.3 THz. Notice that the frequency range has been binned in linear scale. We have checked that binning in logarithmic space or changing the size of the bin does not significantly affects the results.

To understand the range of frequencies for which the universal law (1) is expected to hold, we note that for the smallest system with $N = 222$ (cf. Fig. (1) this range extends up to $\omega \approx 0.4$. For the larger systems the range is smaller, up to about $\omega \approx 0.3$ for $N = 1032$, becoming smallest for $N = 4008$ where it ends just about $\omega \approx 0.2$. We show now that this is due to the invasion of extended modes which do not belong to the quasilocalized modes of interest. To establish this we compute the participation ratio of all the modes, and present the results in Fig. 2. The participation ratio PR is defined as usual [5],

$$PR = \left[N \sum_i (\mathbf{e}_i \cdot \mathbf{e}_i)^2 \right]^{-1}, \qquad (3)$$

where $\mathbf{e}_i$ is the ith element of a given eigenvector of the Hessian matrix. Quasilocalized modes are characterized by a low participation ratio, below $PR \approx 0.2$, whereas fully extended modes have $PR = O(1)$. We note that the cutoff $PR \approx 0.2$ is somewhat *ad hoc*, since very localized modes have a participation ratio of the order $1/N$, whereas the range of interest of quasilocalized modes includes somewhat larger participation ratios. Examining Fig. 2, we see
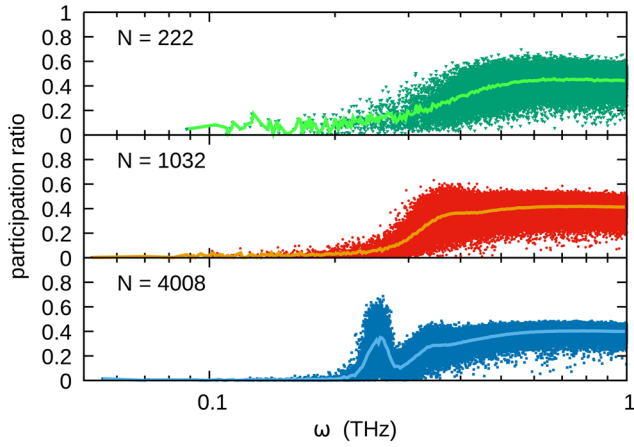
FIG. 2. Participation ratio of all the modes whose frequency $\omega < 1$ as a function of the frequency. The highlighted line is the average over the participation ratios of modes in the same band of frequencies.

that for $N = 222$ modes with $PR < 0.2$ go all the way to $\omega \approx 0.4$ whereas for $N = 1032$ and $N = 4008$ the range ends around $\omega \approx 0.3$ and $\omega \approx 0.2$, respectively. This appears to correlate very nicely with the range of scaling seen in Fig. (1).

An example of very localized mode, corresponding to the smallest ω value for a typical configuration with the largest $N = 4008$, is shown in Fig. 3. This eigenvector is associated to an $\omega = 0.122$ THz, and a participation ratio $PR = 0.00111 \sim 4/4008$, meaning that on average just one thousandth of the atoms is involved by this mode.

To further solidify the universal scaling behavior of the low frequency quasilocalized modes, we turn now to extremal statistics. Since we have many configurations in our simulations, we can determine the minimal frequency obtained
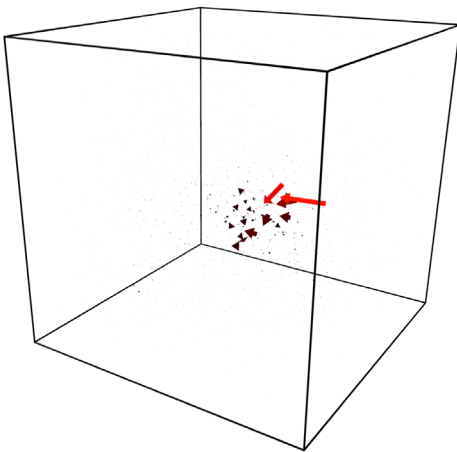

FIG. 3. Orthogonal view of the eigenvector corresponding to $\omega_{\min}$, for a typical configuration with $N = 4008$. Arrows are colored with respect to the modulus e of the vectors, from black ($e = 0$) to red ($e = 0.6$). Arrows have been magnified by a factor of 10.
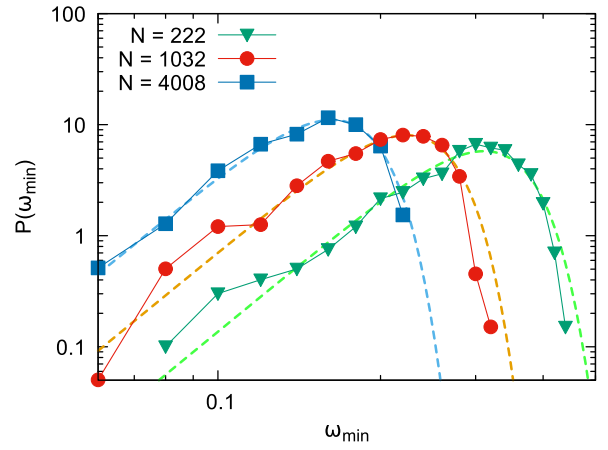

FIG. 4. Distribution of the minimal vibrational frequency $P(\omega_{\min})$ for the three investigated sizes. The dashed lines are the corresponding Weibull distribution Eq. (6).

from the diagonalization of the Hessian matrix in each and every configuration, denoting it as $\omega_{\min}$. The average of this minimal frequency over the ensemble of configurations is $\langle \omega_{\min} \rangle$. Referring to the argument first presented in Ref. [26], we expect that in systems with N particles,

$$\int_0^{\langle \omega_{\min} \rangle} D(\omega) d\omega \sim N^{-1}. \tag{4}$$

Using Eq. (1) we then expect that in three dimensions

$$\langle \omega_{\min} \rangle \sim N^{-1/5} \sim L^{-3/5}. \tag{5}$$

Moreover, since the different realization are uncorrelated, the values of $\omega_{\min}$ are also uncorrelated. Then the celebrated Weibull theorem [27] predicts that the distribution of $\omega_{\min}$ should obey the Weibull distribution

$$W(\omega_{\min}) = \frac{5}{\langle \omega_{\min} \rangle^5} \omega_{\min}^4 e^{-(\omega_{\min}/\langle \omega_{\min} \rangle)^5}. \tag{6}$$
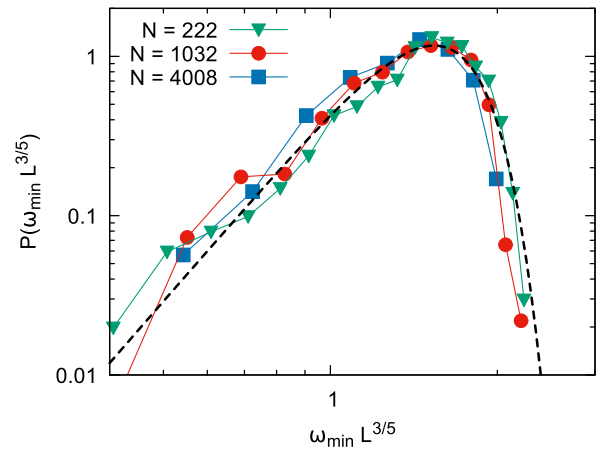

FIG. 5. Distribution of the minimal vibrational frequency $P(\omega_{\min})$ plotted as a function of the rescaled frequency $\omega L^{\frac{3}{5}}$. The dashed black line represents the Weibull distribution.

Indeed, in Fig. 4 the distribution of $\omega_{\min}$ for the three system size is shown, together with the expected distribution Eq. (6). Finally, the scaling shown by Eq. (5) indicates that these distribution can be collapsed by plotting them as a function of the rescaled minimal frequency $\omega_{\min}L^{3/5}$. The rescaling of the curves by $L^{3/5}$ is reported in Fig. 5.

Summary and conclusions.—The main aim of the Letter was to examine whether the universality class that is expressed in Eq. (1) extends beyond glass formers with binary interactions. As already mentioned, quite convincing theoretical considerations predict that this universality class should be wider [1–4]. Hybridization of the glassy quasi-localized modes with regular phonon extended modes obscured for a long time the validity of Eq. (1) for the former. By considering small systems, this hybridization can be avoided, exposing the universal nature of the density of states of the quasilocalized modes. The results presented above show that a structural glass-like silica, with many-body interactions much exceeding the spherical symmetry, also exhibits a dependence of the density of quasilocalized modes on their frequency according to Eq. (1).

We note that this and other demonstrations of the universal law Eq. (1) are achieved in athermal glasses at $T = 0$. A separate discussion is necessary for a thermal system. In that case, the configurations involved are time dependent, and there is a question on which Hessian is appropriate for describing the relevant modes. Some ideas relevant to this question are presented in Ref. [22], but the computation of the density of states remains a task for future research.

[1] U. Buchenau, Yu. M. Galperin, V. L. Gurevich, and H. R. Schober, Anharmonic potentials and vibrational localization in glasses, Phys. Rev. B **43**, 5039 (1991).

[2] V. Gurarie and J. T. Chalker, Bosonic excitations in random media, Phys. Rev. B **68**, 134207 (2003).

[3] V. L. Gurevich, D. A. Parshin, and H. R. Schober, Anharmonicity, vibrational instability, and the boson peak in glasses, Phys. Rev. B **67**, 094203 (2003).

[4] D. A. Parshin, H. R. Schober, and V. L. Gurevich, Vibrational instability, two-level systems, and the boson peak in glasses, Phys. Rev. B **76**, 064206 (2007).

[5] E. Lerner, G. Düring, and E. Bouchbinder, Statistics and Properties of Low-Frequency Vibrational Modes in Structural Glasses, Phys. Rev. Lett. **117**, 035501 (2016).

[6] M. Baity-Jesi, V. Martín-Mayor, G. Parisi, and S. Perez-Gaviro, Soft Modes, Localization, and Two-Level Systems in Spin Glasses, Phys. Rev. Lett. **115**, 267205 (2015).

[7] M. Shimada, H. Mizuno, M. Wyart, and A. Ikeda, Spatial structure of quasilocalized vibrations in nearly jammed amorphous solids, Phys. Rev. E **98**, 060901(R) (2018).

[8] A. Moriel, G. Kapteijns, C. Rainone, J. Zylberg, E. Lerner, and E. Bouchbinder, Wave attenuation in glasses: Rayleigh and generalized-Rayleigh scattering scaling, J. Chem. Phys. **151**, 104503 (2019).

[9] L. Angelani, M. Paoluzzi, G. Parisi, and G. Ruocco, Probing the non-Debye low-frequency excitations in glasses through random pinning, Proc. Natl. Acad. Sci. U.S.A. **115**, 8700 (2018).

[10] Hideyuki Mizuno, Hayato Shiba, and Atsushi Ikeda, Continuum limit of the vibrational properties of amorphous solids. Proc. Natl. Acad. Sci. U.S.A. **114**, E9767 (2017).

[11] Geert Kapteijns, Eran Bouchbinder, and Edan Lerner, Universal Nonphononic Density of States in 2D, 3D, and 4D Glasses, Phys. Rev. Lett. **121**, 055501 (2018).

[12] D. Richard, K. González-López, G. Kapteijns, R. Pater, T. Vaknin, E. Bouchbinder, and E. Lerner, following Letter, Universality of the Nonphononic Vibrational Spectrum across Different Classes of Computer Glasses, Phys. Rev. Lett. **125**, 085502 (2020).

[13] T. Watanabe, D. Yamasaki, K. Tatsumura, and I. Ohdomari, Improved interatomic potential for stressed Si, O mixed systems, Appl. Surf. Sci. **234**, 207 (2004).

[14] Silvia Bonfanti, Ezequiel E. Ferrero, Alessandro L. Sellerio, Roberto Guerra, and Stefano Zapperi, Damage accumulation in silica glass nanofibers, Nano Lett. **18**, 4100 (2018).

[15] S. Bonfanti, R. Guerra, C. Mondal, I. Procaccia, and S. Zapperi, Elementary plastic events in amorphous silica, Phys. Rev. E **100**, 060602 (2019).

[16] See Supplemental Material at http://link.aps.org/supplemental/10.1103/PhysRevLett.125.085501 for description of the employed Watanabe's potential and parameters.

[17] E. Bitzek, P. Koskinen, F. Gähler, M. Moseler, and P. Gumbsch, Structural Relaxation made Simple, Phys. Rev. Lett. **97**, 170201 (2006).

[18] R. Brueckner, Properties and structure of vitreous silica. I, J. Non-Cryst. Solids **5**, 123 (1970).

[19] K. Vollmayr-Lee and A. Zippelius, Temperature-dependent defect dynamics in the network glass SiO 2, Phys. Rev. E **88**, 052145 (2013).

[20] D. L. Malandro and D. J. Lacks, Relationships of shear-induced changes in the potential energy landscape to the mechanical properties of ductile glasses, J. Chem. Phys. **110**, 4593 (1999).

[21] C. E. Maloney and A. Lemaître, Amorphous systems in athermal, quasistatic shear, Phys. Rev. E **74**, 016118 (2006).

[22] P. Das, V. Ilyin, and I. Procaccia, Instabilities of time-averaged configurations in thermal glasses, Phys. Rev. E **100**, 062103 (2019).

[23] For systems at finite temperature special considerations are necessary, see, for example, Ref. [22].

[24] S. Plimpton, Fast parallel algorithms for short-range molecular dynamics, J. Comput. Phys. **117**, 1 (1995).

[25] A. Stukowski, Visualization and analysis of atomistic simulation data with OVITO–the Open Visualization Tool, Model. Simul. Mater. Sci. Eng. **18**, 015012 (2010).

[26] S. Karmakar, E. Lerner, and I. Procaccia, Statistical physics of the yielding transition in amorphous solids, Phys. Rev. E **82**, 055103(R) (2010).

[27] W. Weibull, A statistical theory of the strength of materials, Generalstabens litografiska anstalts förlag, Stockholm, 1939.